

## Use of Bioballs as an Adsorbent for the Removal of Copper

Hakan Çelebi

Department of Environmental Engineering, Aksaray University, 68100, Aksaray, TURKEY.  
hakanaz.celebi@gmail.com

(Received on 10th May 2020, accepted in revised form 20<sup>th</sup> October 2020)

**Summary:** Nowadays, heavy metals, which are among the various hazardous pollutants, are present at a high level of density in the receiving environments. Among heavy metals, especially copper is mainly present in wastewater due to the industrial activities. Adsorption is the most practical method to prevent this pollution, and in recent years, researchers have been involved in researching both adsorption and cost-efficient, accessible, easy-to-apply environmentally friendly adsorbents. In this study, the adsorption capacity of high density bioballs having a potential adsorbent characteristic was investigated. Accordingly, different pH values (2.0 – 6.0) and the contact times (1 -150 minutes) of a solution on the adsorption process was evaluated under a constant agitating speed (150 rpm), a constant temperature (25°C) and a fixed amount of adsorbent (2.0 g). Experimental data on the pH and contact times obtained were evaluated using different isotherm and kinetic models in a batch process. The optimum conditions for the adsorption process were determined as follows: adsorbent dose = 2 g/L, pH = 6.23 and contact time = 45 minute. The maximum copper refining efficiency of a high density bioball was calculated to be approximately 78% under the optimum conditions determined. The maximum adsorption capacity based on the Langmuir isotherm is 5.60 mg/g, and the adsorption of the copper element onto the high-density bioball is defined by a pseudo-second-order kinetics. The process was found to be applicable, spontaneous, and endothermic according to thermodynamic parameters. As a result, it has been noted that high density bioballs used as a biofilm material may be an alternative adsorbent for copper and the other heavy metals.

**Keywords:** Adsorption, Adsorbent, Heavy metal, Copper, Bio ball.

### Introduction

Rapid industrialization, urbanization and the discharge of heavy metals into water caused by the technological progress have attracted many researchers' attention due to their toxicities and carcinogenic effects. In particular, water pollution caused by heavy metal ions leads to serious environmental hazards and waterborne diseases. Heavy metals are the elements having a high density in the range of 3.5 to 7 g/cm<sup>3</sup> and an atomic weight between 63.5 and 200.6 g/mol and have harmful effects at low concentrations [1]. They are mostly found in the earth's crust and are not biodegradable, thus they are bio accumulative. Due to these features, they accumulate in living organisms and cause various health problems (neurological disorders, cancer, organ failure, kidney and lung damage, digestive system problems, skin lesions, etc.). The main sources of heavy metal ions include resources such as mining, vehicle emissions, agricultural flow, industrial waste, fossil fuel burning, welding processes, and electroplating [2]. The most dangerous heavy metal ions in the world are listed as cadmium (Cd<sup>2+</sup>), arsenic (As<sup>3+</sup>/As<sup>5+</sup>), mercury (Hg<sup>2+</sup>), chromium (Cr<sup>6+</sup>), lead (Pb<sup>2+</sup>), and copper (Cu<sup>2+</sup>) [3].

Cu<sup>2+</sup> is one of the pollutants found in the receiving mediums that cause risk for ecology and human health [1]. Copper is found in the receiving environments as Cu<sup>0</sup>, Cu<sup>+</sup> and Cu<sup>2+</sup>, but it also causes health problems such as stomachache, headache, nausea, kidney damage, skin irritation, and depression [4]. However, it is a heavy metal that is in high demand

due to its economic importance. Cu<sup>2+</sup> is used extensively in the energy, material, and transportation sectors due to its original physicochemical structure. It is well known that Cu<sup>2+</sup> is an element formed in all water environments on a global scale [5]. The main anthropogenic copper resources are industrial (painting, metalwork, mining processes, refining processes, batteries and electronics manufacturing, textile and nuclear energy, etc.), domestic (leachate, wastewater treatment plants, etc.) and agricultural (treatment sludge applications, fertilization, etc.) activities. Cu<sup>2+</sup>, which is released as a result of these activities, may mix with air, soil and especially water and cause significant environmental changes [6]. Therefore, removal of Cu<sup>2+</sup> is important for protecting human beings and their environment. According to the World Health Organization (WHO), the permissible limit for Cu<sup>2+</sup> in drinking water is 2.0 mg/L, while the United States Environmental Protection Agency (USEPA) has determined the content of Cu<sup>2+</sup> in industrial wastewater as 1.3 mg/L [7].

There are different methods for removing Cu<sup>2+</sup> from different receiving water environments. These include chemical deposition, ion exchange, adsorption, membrane, reverse osmosis and electrodeposition, which are commonly applied methods [8,9]. However, apart from adsorption, these technologies have many disadvantages such as their requirements for expensive chemicals, low removal efficiencies and secondary wastes in the treatment process. Among the reported methods for removing Cu<sup>2+</sup>, adsorption is the most

---

\*To whom all correspondence should be addressed.

preferred process due to its pure and rapid process, maximum efficiency, simple configuration, easy regeneration, proper preparation, remarkable recycling performance, relatively low cost and availability in low concentration  $\text{Cu}^{2+}$  aqueous environments [10]. Many adsorbents (agricultural and industrial solid wastes, resins, fibers, activated carbon, chitosan, functional polymers, nanomaterials, different clay groups, etc.) have been used to extract  $\text{Cu}^{2+}$  from the aqueous solution [1, 11].

Bioballs are generally used in freshwater or saltwater aquariums, various non-swimming pools, biofilm layer formation in anaerobic/aerobic reactors in the wastewater treatment and biological filtration. These bioballs contribute to the removal of harmful pollutants in the water by allowing the microorganisms that support the treatment to grow and colonize thereon. These materials are generally made of thermal- and chemical corrosion-resistant materials based on polymer and plastic (polyhedral, polyethylene, polypropylene, reinforced polypropylene, polyvinyl chloride, chlorinated polyvinyl chloride, etc.). The properties of polymer and plastic adsorbents include adjustable surface chemistry, large surface area, pore size distribution, excellent mechanical strength and easy production [12]. These properties render the bioballs excellent materials that are suitable for the removal of the pollutants such as heavy metals, dyes, etc. from water environments. Although there are many studies on heavy metal adsorption in the literature, this research differs from other studies in terms of the material used. Because in the other studies, powdered or granular polymer or plastic materials can be applied to adsorption with modifications, whereas in our study, bioballs which are generally used as biofilm support materials in aquarium cleaning and treatment processes were used as adsorbents in an integral form during the adsorption process for the first time. With this study, the removal of heavy metals, which pose major problems in terms of

environment and human health, using different materials other than activated carbon, has been investigated. In the study, removal of  $\text{Cu}^{2+}$  from water was aimed by using the adsorption method, which is economic and has high removal efficiency. In the study conducted according to the batch method, high density bioballs (Hi-DBB) were used as an adsorbent.

## Experimental

To prepare a  $\text{Cu}^{2+}$  solution (100 mg/L), 3.928 g of  $\text{CuSO}_4 \cdot 5\text{H}_2\text{O}$  compound was dissolved in 1 L of pure water (chemical resistance: 18  $\text{M}\Omega \text{ cm}$ ; 1.2  $\mu\text{g/L}$  of total organic carbon), and a 1 L solution of  $\text{Cu}^{2+}$  was prepared. All chemicals used are of more than 97% analytical purity and were purchased from Merck GmbH (Darmstadt, Germany). The pH balance of the solutions used in the experiments was adjusted with 0.01 M NaOH or 0.01 M HCl when necessary. The pH measurements were performed with a combination electrode with a LABQUEST2 digital ion analyzer. Mixing operations for the solutions were carried out using the analytical model ZHWY-200B, ZHICHENG benchtop incubator shaker at a constant stirring speed of 150 rpm and a constant temperature of 25 °C. Commercial bioballs produced in different sizes by various companies were purchased ready-made in this study. High-density bio balls have been preferred because they are both easily accessible and economical. A Hi-DBB material with dimensions of 4.88 x 3.98 x 3.35 cm and a minimum weight of 2 g was applied in the batch adsorption experiments. Hi-DBB adsorbent is generally produced from polyvinyl chloride (PVC) material and the elemental analysis results for PVC are given in Table-1 [13].

Table-1: Element distribution of PVC material.

Material	Element composition (wt.%)							
PVC	C	O	Cl	Mg	Al	Ca	Si	S
	57±6	4±0.6	37±9	≤0.01	0.6±0.1	1.3±0.1	0.1±0.01	0.02±0.01



Fig. 1: Schematic representation of the adsorption of  $\text{Cu}^{2+}$  on Hi-DBB.

Adsorption tests were carried out in glass equipment according to the batch method. 250 mL sealed Erlenmeyer flasks with a working volume of 100 mL were used. Schematic representation of the adsorption of  $\text{Cu}^{2+}$  onto the Hi-DBB is shown in Fig. 1. Experiments were carried out under suitable conditions according to pH and contact time parameters, which determine the basic mechanism for the adsorption test. Unlike the studies in the literature, the parameter adsorbent amount was not included in the effect factors since it is not in a powder or granular form. In the study, the Hi-DBB, the adsorption efficiency of which will be determined, was used in an integral form, and a fixed amount of Hi-DBB (2.0 g) was used in all experiments. The samples filtered to calculate the amount adsorbed were placed in an “ICP-OES, 2100DV, Perkin Elmer, USA” inductively coupled plasma optical emission spectrometer (ICP-OES), and the results were recorded (Fig. 1). After the adsorption reaches equilibrium, the percentage of copper adsorption “A (%)” and  $\text{Cu}^{2+}$  adsorption capacity “ $q_e$  (mg/g)” per unit amount of the Hi-DBB are calculated by the following formulas. Wherein; A:  $\text{Cu}^{2+}$  removal efficiency (%),  $C_0$  and  $C_e$ : initial and final concentrations of  $\text{Cu}^{2+}$  (mg/L), m: amount of Hi-DBB (mg), V: volume of solution (mL),  $q_e$ : experimental amount of  $\text{Cu}^{2+}$  adsorbed by the Hi-DBB (mg/g).

$$q_e = \frac{(C_0 - C_e) \times V}{1000 \times m} \quad (1)$$

$$A (\%) = \frac{(C_0 - C_e)}{C_0} \times 100 \quad (2)$$

## Results and Discussion

### Optimum Contact Time

The contact time is the time required for the adsorption process to reach equilibrium, and when adsorption studies with  $\text{Cu}^{2+}$  are examined, the adsorption balance can generally occur in long periods of time. Fig. 2 shows the contact time relationship between Hi-DBB and  $\text{Cu}^{2+}$ .  $\text{Cu}^{2+}$  adsorption was investigated on Hi-DBB as a function of time in the range of 5-120 minutes. Efficiency initially showed a slight increase within the first 15 minutes' period, while the increase gained speed from the 30<sup>th</sup> minute. For Hi-DBB, the maximum removal efficiency of  $\text{Cu}^{2+}$  has reached 77.45% within 45-minute contact time. The removal rate of 15.68% to 77.45% within the first 45 minutes of the adsorption process may result from the larger free surface area of Hi-DBB for  $\text{Cu}^{2+}$  adsorption. In addition, it can be said that the composition and pore size of Hi-DBB made of polymer or plastic material

examined may affect adsorption. The findings of many studies in the previous literature are consistent with the results of the study (Table-4) [14-16].

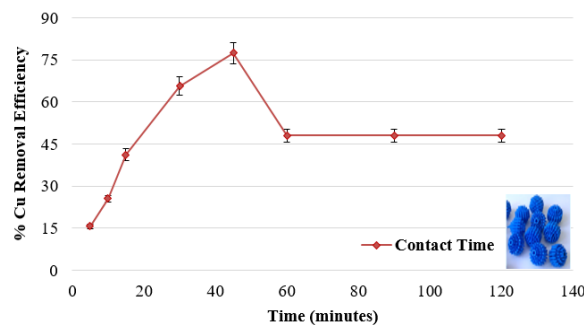


Fig. 2: Effect of time on removal of  $\text{Cu}^{2+}$  by Hi-DBB ( $\text{Cu}^{2+}$  initial: 100 mg/L, Hi-DBB dose: 2 g, pH: 6.23, 25 °C).

### Optimum pH

pH is an environmental parameter and is the most important factor affecting the adsorption. pH can affect both the adsorbent and the structure adsorbed. As the pH changes, the adsorption efficiency changes as the hydrogen ( $\text{H}^+$ ), hydroxyl ( $\text{OH}^-$ ) ions in the environment change strongly. In Fig. 3, it is seen that Hi-DBB affects the adsorption of  $\text{Cu}^{2+}$  in the pH ranges of 2 to 9. As a result of batch experiments between different pH values, the maximum  $\text{Cu}^{2+}$  removal efficiency (78.43%) was found at pH 6.23. The maximum  $\text{Cu}^{2+}$  efficiency recorded for the pH environment of 6.23 may be the result of the interaction between the  $\text{H}^+$  and  $\text{OH}^-$  ions in the solution and the functional groups in the adsorption zones of Hi-DBB. It is also a known fact that the adsorption efficiency depends to the charge of the adsorbent surface. As a result of the studies, it has been stated that the most suitable pH values for  $\text{Cu}^{2+}$  adsorption of polymer and plastic materials are between 5 and 6.9 [17]. The adsorption capacities are decreased for the materials of this nature at a low pH (very acidic) and a pH above 7. This is because pH affects the degree of ionization and the adsorbent surface. When the pH is lower than 4, the acidity will be high due to the positive charge and electrostatic repulsion. In this case, it will reduce the adhesion of positively charged  $\text{Cu}^{2+}$  [1]. Therefore, there will be a decrease in the number of negatively charged areas to bind  $\text{Cu}^{2+}$  due to the protonation of the active sites. Most heavy metals tend to precipitate at high pH values. However, the optimum pH value for Cu adsorption with HDBB was found to be 6.23 that adsorption takes place efficiently. Pourbaix diagrams were used to properly evaluate the metal diversity of Cu in the water samples subjected to chemical

analysis. It was observed that for Cu analyzed, there was a large overlap between the chemical species predicted by the Pourbaix diagrams [18]. The predominant species Cu in the aqueous phase depends on the pH and Pourbaix diagram. The main species present at  $\text{pH} \leq 6$  are  $\text{Cu}^{2+}$ ,  $\text{Cu}^+$  while at  $\text{pH} \geq 7$  are  $\text{Cu}(\text{OH})_2$  and  $\text{Cu}_2\text{O}$  [18]. In this study, the pH values were adjusted to be in the range of 2.0-9.0. As heavy metals cannot dissolve at neutral or basic pH values, determining the degree of metal contamination in water at  $\text{pH} \geq 7$  can be misleading. After pH 7, the formation precipitation of heavy metal ions as their own hydroxides may affect the adsorption results, therefore adsorption experiments were conducted in the pH range of 2-9. Because, the study was continued until high pH values in order to see clearly the distinction between adsorption and chemical precipitation. Thus, the efficiency of the adsorption process was observed in accordance with the purpose of the study. According to the Pourbaix diagram of Cu, the  $\text{Cu}^{2+}$  ions precipitated as  $\text{Cu}(\text{OH})_2$  at pH values greater than 6 [18]. Some studies have indicated that the maximum copper adsorption is at about pH 6 [19].

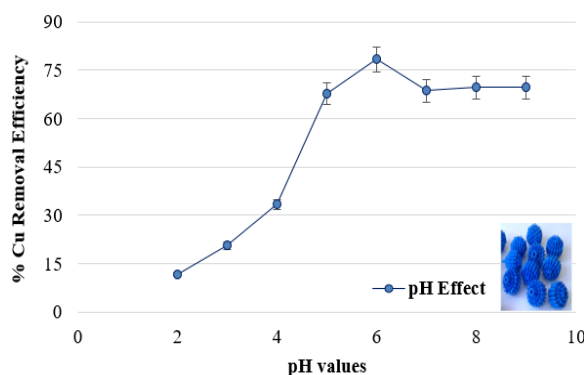


Fig. 3: Effect of pH on removal of  $\text{Cu}^{2+}$  by Hi-DBB ( $\text{Cu}^{2+}_{\text{initial}}$ : 100 mg/L, Hi-DBB dose: 2 g, pH: 6.23, 25 °C).

#### Effect of mixing speed

Fig. 4 shows the effect of mixing speed on  $\text{Cu}^{2+}$  removal. Experiments were carried out at 50, 100, 150, 200, 250, 300, and 350 rpm mixing speeds to determine the effect of mixing speed on adsorption when removing  $\text{Cu}^{2+}$  from Hi-DBB from the aqueous solution. As a result of the experiments,  $\text{Cu}^{2+}$  removal efficiencies were calculated as 58.25, 81.2, and 64.5%, respectively. Fig. 4 shows that  $\text{Cu}^{2+}$  removal increases at mixing speeds in the range of 50-150 rpm, and maximum efficiency is achieved at 150 rpm. This is due to the fact that  $\text{Cu}^{2+}$  ions come in contact with the active porous inner surface regions

of Hi-DBB together with increasing speed. At low and high mixing speeds,  $\text{Cu}^{2+}$  treatment was lower than the optimum value of 150 rpm. Low mixing speeds (50 and 100 rpm) cannot provide the energy required for  $\text{Cu}^{2+}$  ions to attach to the surface of the Hi-DBB [20]. On the other hand, at high mixing speeds (200, 250, 300, and 350 rpm), there is not enough contact time to connect  $\text{Cu}^{2+}$  ions to Hi-DBB.

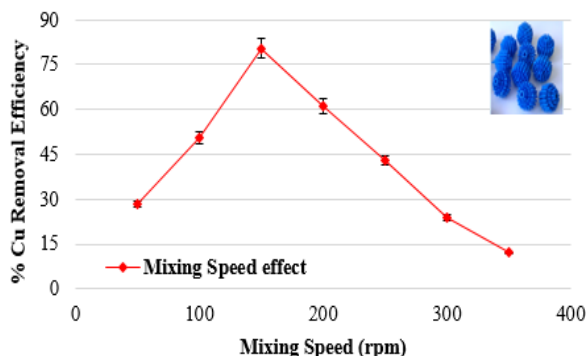


Fig. 4: Effect of mixing speed on removal of  $\text{Cu}^{2+}$  by Hi-DBB ( $\text{Cu}^{2+}_{\text{initial}}$ : 100 mg/L, Hi-DBB dose: 2 g, pH: 6.23, 25 °C).

#### Thermodynamic effects of temperature changes

Temperature is one of the parameters that play a role in every chemical reaction. Temperature affects the solubility and stability of metal ions. As a result, the temperature effect on thermodynamics and reaction kinetics may have a non-linear variable (positive-negative) effect. However, some researchers suggest that the effect of temperature is smaller than the impact of parameters such as adsorbent dose, pH, and contact time. Each adsorbent and metal ion must be specifically tested to identify the effect of temperature on the overall adsorption process. In this study, there were no major differences in Cu removal efficiencies at three different temperatures (298, 308 and 318 K) values (data not shown). Therefore, when evaluating the effect of temperature in the removal of heavy metals, thermodynamic parameters should be tested. When evaluating the effect of temperature in the removal of heavy metals, thermodynamic parameters should be tested. Thermodynamic parameters are important factors for determining the level of spontaneous formation of adsorption and energy need. Thermodynamic parameters (Gibbs energy,  $\Delta G^\circ$  (kJ / mol), standard entropy change,  $\Delta S^\circ$  (J / mol / K), standard enthalpy change,  $\Delta H^\circ$  (kJ / mol)) are determined using equations 3 and 4.  $K_d$  is the thermodynamic distribution coefficient and was calculated using equation 5 [14].

$$\Delta G^\circ = -RT \ln K_d \quad (3)$$

R [8.314 (J/mol/K)] and  $K_d$ : thermodynamic distribution coefficients

$$\ln K_d = \frac{\Delta S^\circ}{R} - \frac{\Delta H^\circ}{RT} \quad (4)$$

$$K_d = \frac{q_e}{C_e} \quad (5)$$

The  $\Delta G^\circ$  values calculated according to temperature changes and  $K_d$  values are given in Fig. 5 and Table-2. All  $\Delta G^\circ$  values are negative, which clearly reveals the spontaneous adsorption studies in the batch system. In addition, negative values of  $\Delta G^\circ$  indicate that the bond energy between Hi-DBB and  $\text{Cu}^{2+}$  is strong. According to the literature,  $\Delta G^\circ$  is between zero and -20 kJ/mol for physical adsorption, and -80 and -400 kJ/mol for chemical adsorption. In  $\text{Cu}^{2+}$  treatment with Hi-DBB,  $\Delta G^\circ$  remained below -20 and the limit value was not exceeded despite the temperature increase. Positive values of  $\Delta H^\circ$  and  $\Delta S^\circ$  show that  $\text{Cu}^{2+}$  adsorption is endothermic and randomness increases between  $\text{Cu}^{2+}$  solutions in active regions of Hi-DBB. As the temperature increases, the degree of self-realization of the process increases. Also,  $\Delta H^\circ$  16.47 kJ/mol positive value for  $\text{Cu}^{2+}$  adsorption indicates that adsorption to Hi-DBB are endothermic in physical sorption. The positive result of  $\Delta S^\circ$  (3.76 J/mol/K) is the interaction of Hi-DBB and  $\text{Cu}^{2+}$  in the solid-liquid interface. The findings of many studies in the previous literature are consistent with the results of the study [7, 20]. In addition, some studies have stated that adsorption is exothermic [21].

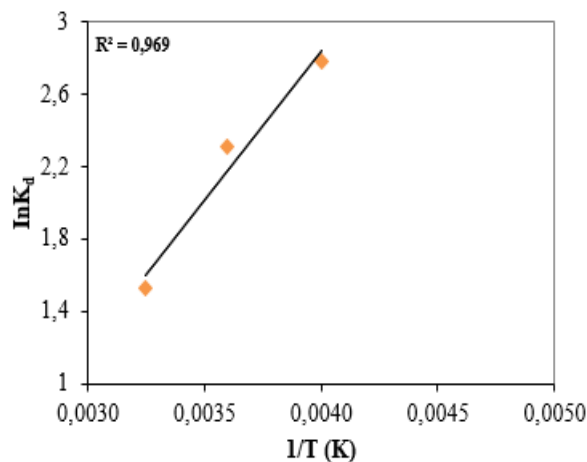


Fig. 5: The adsorption thermodynamic of  $\text{Cu}^{2+}$  ions onto Hi-DBB.

Table-2: Thermodynamic constants for the adsorption of  $\text{Cu}^{2+}$  onto Hi-DBB.

Metal	$\Delta G^\circ_{298}$ (kJ/mol)	$\Delta G^\circ_{308}$ (kJ/mol)	$\Delta G^\circ_{318}$ (kJ/mol)	$\Delta H^\circ$ (kJ/mol)	$\Delta S^\circ$ (J/mol/K)
$\text{Cu}^{2+}$	-5.72	-6.03	-6.17	16.47	3.76

*Isotherm and kinetic models applied in the batch experiments*

In the batch system, four groups of isotherms were applied to detect adsorption. The coefficients, correlation factors ( $R^2$ ) and mathematical equations for the isotherm parameters obtained are listed in Table-3 [48-53]. Also, the main properties of a Langmuir isotherm may be expressed by the dimensionless constant separation factor ( $R_L$ ). The  $R_L$  parameter shows the shape of the isotherm as follows:  $R_L > 1$ , unfavorable;  $R_L = 1$ , linear;  $0 < R_L < 1$ , favourable and  $R_L = 0$ , irreversible. The calculated maximum adsorption capacity ( $q_m$ ) was determined as 5.60 mg/g at 25°C, with a contact time of 45 minutes and an initial  $\text{Cu}^{2+}$  concentration of 102 mg/L. Fig. 6 and Fig. 7 show the suitability of Langmuir, Freundlich, Dubinin-Radushkevich (D-R), and Temkin isotherms in the  $\text{Cu}^{2+}$  adsorption system to laboratory-scale results. As can be seen in Table-3, the Langmuir model gave the best experimental result for  $\text{Cu}^{2+}$  adsorption on Hi-DBB due to the highest correlation coefficient ( $R^2=0.781$ ). The dimensionless constant separation factor ( $R_L$ ) was 0.022 for the initial copper concentration of 102 mg/L, and showed suitable adsorption for Langmuir in the range of  $0 < R_L < 1$ . However, other models have a poor inconsistency. These results are in line with the results of previous studies [28].

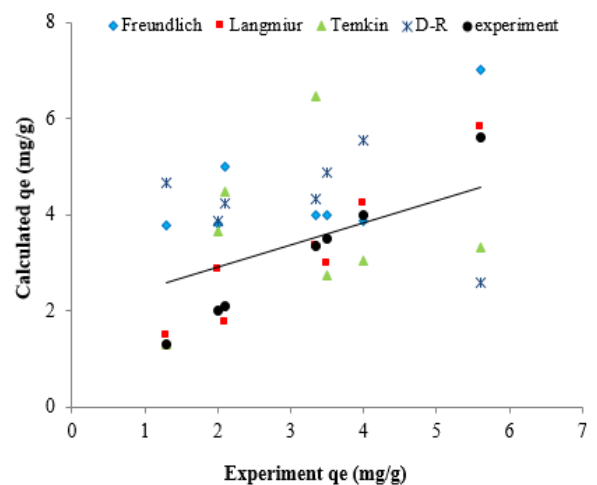


Fig. 6: Experimental and calculated isotherm curves in the adsorption system



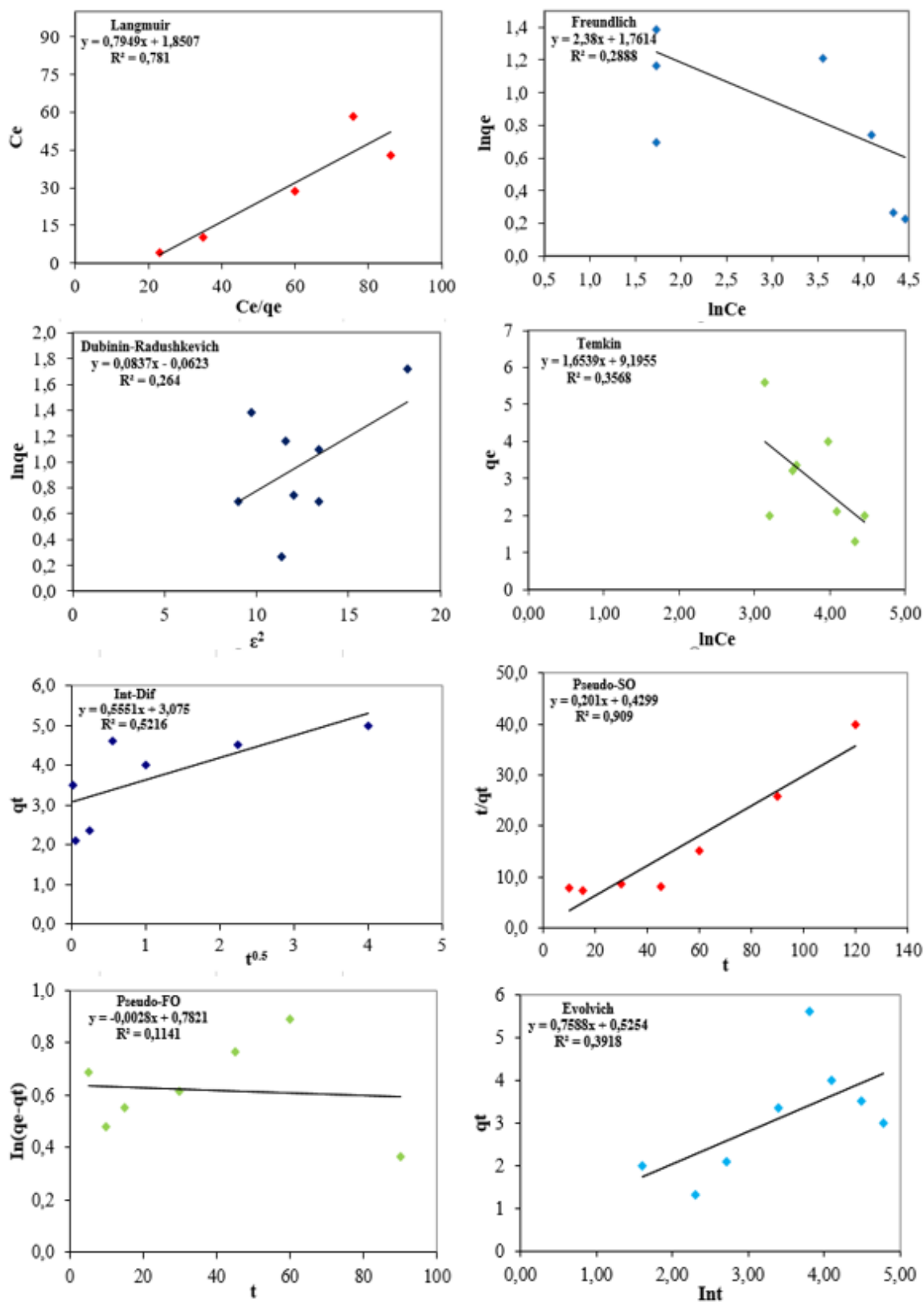
Fig. 7: Isotherm and kinetic curves of  $\text{Cu}^{2+}$  adsorption with Hi-DBB.

Table-3: Isotherm models, their linear forms and respective coefficient.

Models	Equations	Description	Coefficients	
Langmuir	$q_e = \frac{q_m K_L C_e}{1 + K_L C_e}$ $R_L = \frac{1}{1 + K_L \times C_e}$	$q_m$ : maximum adsorption capacity; $K_L$ : density constant; $R_L$ : Separation factor: $R_L > 1$ : unfavorable; $R_L = 1$ : linear; $R_L = 0$ : irreversible; $0 < R_L < 1$ : favorable	$q_m$ (mg/g) $K_L$ (L/mg) $R_L$ $R^2$	5.60 0.43 0.02 0.78
Freundlich	$q_e = K_F \sqrt[n]{C_e}$	$K_F$ : adsorption capacity; $n$ : intensity of adsorption; $1/n = 0$ irreversible; $1/n > 1$ unfavorable; $0 < 1/n < 1$ favorable	$K_F$ (mg/g) $n$ $R^2$	5.82 0.42 0.29
Tempkin	$q_e = q_m \ln[(K_T)C_e]$	$K_T$ : Equilibrium constant	$K_T$ (L/mg) $R^2$	260 0.36
D-R	$\ln q_e = \ln q_{\max} - \beta \epsilon^2$	$B$ : Equilibrium constant; $\epsilon$ : Polanyi potential	$\beta$ (mol <sup>2</sup> /J <sup>2</sup> ) $E$ (kJ/mol) $R^2$	0.08 2.44 0.26
PFO	$\ln(q_e - q_t) = \ln q_e - k_1 t$	$k_1$ : PFO kinetic constant	$k_1$ (1/min) $q_e$ (mg/g) $R^2$	0.01 1.67 0.32
PSO	$\frac{t}{q_t} = \frac{1}{k_2 \times q_e^2} + \frac{1}{q_w} t$	$k_2$ : PSO kinetic constant	$k_2$ (g/mg/min) $q_e$ (mg/g) $R^2$	0.20 4.98 0.91
Int-Dif	$q_t = k_d \times t^{0.5}$	$k_d$ : Rate coefficient of Int-Dif	$k_d$ $R^2$	0.56 0.52
Elovich	$q_t = \frac{1}{\beta} \ln \alpha \beta + \frac{1}{\beta} \ln t$	$\alpha, \beta$ : Elovich constants	$\alpha$ $\beta$ $R^2$	2.63 0.76 0.39

Table-4: Comparison of Cu<sup>2+</sup> adsorption criteria of some plastic and polymer based adsorbents.

Adsorbent	Optimum Conditions				Parameters				R
	C (mg/L)	pH	T (min)	T (°C)	% Y	AC (mg/g)	I	K	
Amine+silica	150	6.5	1440	25	92	10.41	L	PSO	[32]
Polyaniline+Zr	50	6.0	90	-	96	25.75	-	-	[33]
Polyamine	-	5.0	-	-	85	1.47	-	PSO	[34]
Chitosan+PVC	100	5.0	210	-	68	87.9	L	PSO	[35]
Synthetic materials	-	6.0	20	-	99	0.05	-	-	[36]
Modified PET film	2000	4.0	60	25	-	55.6	L	PSO	[37]
Modified Lignin	-	4.0	240	57	-	20	-	-	[38]
Modified Polymer	10	6.0	120	57	87	31.45	L/F	-	[39]
Polydopamine+Zeolite	100	5.5	1240	-	89	14.95	L	PSO	[40]
Modified Cellulose	300	7.0	30	-	97	70	L	PSO	[41]
Keratin+Polyamid6	35	5.8	1240	-	-	103.5	F	PSO	[42]
Polystyrene	50	5.5	15	20	78	134	L	-	[43]
Fiber+Fe <sub>2</sub> O <sub>3</sub>	30	5.5	60	25	21	4.98	-	PSO	[44]
Modified Silica	10	4.0	140	25	76	41.5	L	PSO	[45]
Silica KIT6	10	5.5	90	20	97	9.03	L	PSO	[46]
Thiol+Polymer	10	4.0	20	-	81	9.43	-	PSO	[47]

C: Initial Concentration; T: Temperature; AC: Adsorption Capacity; T: Time; Y: Yield; I: Isotherms, K: Kinetics; R: References

Adsorption kinetics is important for determining the intake of Cu<sup>2+</sup> on Hi-DBB in the solid-phase interface. In this study, four different kinetic models (pseudo-first-order (PFO), pseudo-second-order (PSO), intraparticle diffusion (Int-Dif) and Elovich) were evaluated to define the batch system (Table-3). Adsorption capacities and values calculated from the models are given in Table-3. When the kinetic data findings are compared, it may be said that the best correlation coefficient is obtained with the PSO model. In addition, the values obtained from the PSO model show that the

adsorption was experimentally successful. According to previous studies focusing on the adsorption of Cu<sup>2+</sup> by different adsorbents, the removal of Cu<sup>2+</sup> is suitable for the PSO kinetic modeling [16]. In addition, the PSO has defined all batch systems and the chemisorption in nature as the limiting factor for all adsorption capacities [29].

Comparison of Cu<sup>2+</sup> removal to different polymer and plastic based adsorbents reported in the literature is given in Table-4. Samadi et al. [30] examined the removal of Cu<sup>2+</sup> from the aqueous

medium using polystyrene and melamine polymer derivatives, and as a result, achieved similar results with our study. As can be seen, the observed treatment efficiencies of Hi-DBB for  $\text{Cu}^{2+}$  are comparable to the other adsorbents [31].

## Conclusion

The current experimental study results have shown that the adsorption of the  $\text{Cu}^{2+}$  element on Hi-DBB depends on the pH and contact time. The maximum purification efficiency of Hi-DBB was achieved as approximately 78% for  $\text{Cu}^{2+}$  under the optimum conditions. Optimum conditions for the adsorption process of Hi-DBB were determined as follows: Hi-DBB dose = 2 g/L, pH = 6.23 and contact time = 45 minutes. The maximum adsorption capacity and the correlation coefficient ( $R^2$ ) based on the Langmuir isotherm are 5.60 mg/g and 0.781, and the adsorption of  $\text{Cu}^{2+}$  on Hi-DBB is defined by the pseudo-second-order kinetics. Thermodynamic parameters ( $\Delta H^\circ$ ,  $\Delta S^\circ$ ,  $\Delta G^\circ$ ) obtained during the adsorption process indicate that Hi-DBB is applicable, spontaneous and endothermic for  $\text{Cu}^{2+}$  adsorption. This study clearly shows that Hi-DBB can be a practical, effective and environmentally friendly alternative adsorbent for the purification of  $\text{Cu}^{2+}$  from aqueous solutions.

## Acknowledgements

The research has not received any financial and technical support, and the author has not reported any conflict of interest. This study was undertaken in the Water Laboratories at Aksaray University Environmental Engineering Department, Aksaray Turkey. I am grateful for the help, feedback, comments, and advice provided by the *Journal of the Chemical Society of Pakistan* editors and referees.

## References

1. R.O. Adeeyo, J.N. Edokpayi, O.S. Bello, A.O. Adeeyo, J.O. Odiyo, Influence of selective conditions on various composite sorbents for enhanced removal of copper (II) ions from aqueous environments, *Int. J. Environ. Res. Public Health*, **16**, 4596 (2019).
2. B.M. Ali, F. Wang, R. Boukherroub, W. Lei, M. Xia, Phytic acid-doped polyaniline nanofibers-clay mineral for efficient adsorption of copper (II) ions, *J. Colloid Interface Sci.*, **553**, 688 (2019).
3. S.B. Ali, I. Jaouali, S.N. Souissi, A. Ouederni, Characterization and adsorption capacity of raw pomegranate peel biosorbent for copper removal, *J. Clean. Prod.*, **142**, 3809 (2017).
4. D. Prabu, R. Parthiban, S.K. Ponnusamy, S. Anbalagan, R. John, T. Titus, Sorption of Cu(II) ions by nano-scale zero valent iron supported on rubber seed shell, *IET Nanobiotechnol.*, **11**, 714 (2017).
5. A. Pugazhendhi, K. Ranganathan, T. Kaliannan, Biosorptive removal of copper (II) by *Bacillus cereus* isolated from contaminated soil of the electroplating industry in India, *Water Air Soil Pollut.*, **229**, 1 (2018).
6. S. Mustapha, D.T. Shuaib, M.M. Ndamitso, M.B. Etsuyankpa, A. Sumaila, U.M. Mohammed, M. B. Nasirudeen, Adsorption isotherm, kinetic and thermodynamic studies for the removal of Pb(II), Cd(II), Zn(II) and Cu(II) ions from aqueous solutions using *Albizia lebbeck* pods, *Appl. Water Sci.*, **9**, 142 (2019).
7. K. Manzoor, M. Ahmad, S. Ahmad, S. Ikram, Synthesis, characterization, kinetics, and thermodynamics of EDTA-modified chitosan-carboxymethyl cellulose as Cu(II) ion adsorbent, *ACS Omega*, **4**, 17425 (2019).
8. N. Wahab, M. Saeed, M. Ibrahim, A. Munir, M. Saleem, M. Zahra, A. Waseem, Synthesis, Characterization, and applications of silk/bentonite clay composite for heavy metal removal from aqueous solution, *Front. Chem.*, **7**, 1 (2019).
9. B.C. Nyamunda, T. Chivhanga, U. Guyo, F. Chigondo, Removal of Zn (II) and Cu (II) ions from industrial wastewaters using magnetic biochar derived from water hyacinth, *Hindawi J. Eng.*, **2019**, 1 (2019).
10. R. Chakraborty, A. Asthana, A.K. Singh, B. Jain, A.B.H. Susan, Adsorption of heavy metal ions by various low-cost adsorbents: a review, *Int. J. Environ. Anal. Chem.*, **in press** (2020).
11. Z. Yang, Y. Chai, L. Zeng, Z. Gao, J. Zhang, H. Ji, Efficient removal of copper ion from wastewater using a stable chitosan gel material, *Molecules*, **24**, 4205 (2019).
12. Y. Hu, Q. Wang, J. Zhao, S. Xie, H. Jiang, A novel porous media permeability model based on fractal theory and ideal particle pore-space geometry assumption, *Energies*, **13**, 510 (2020).
13. I. Turku, S. Kasala, T. Karki, Characterization of polystyrene wastes as potential extruded feedstock filament for 3D printing, *Recycling*, **3**, 57 (2018).
14. H.F. Heiba, A.A. Taha, A.R. Mostafa, L.A. Mohamed, M.A. Fahmy, Synthesis and characterization of CMC/MMT nanocomposite for  $\text{Cu}^{2+}$  sequestration in wastewater treatment, *Korean J. Chem. Eng.*, **35**, 1844, (2018).



15. Y. Niu, W. Yu, Z. Qin, X. Nie, S. Yang, Q. Wan, Adsorption characteristics of copper ion on nanoporous silica, *Acta. Geochim.*, **38**, 517 (2019).
16. R. Shan, Y. Shi, J. Gu, Y. Wang, H. Yuan, Single and competitive adsorption affinity of heavy metals toward peanut shell-derived biochar and its mechanisms in aqueous systems, *Chin. J. Chem. Eng.*, **in press** (2020).
17. A. Adil, S.M. Wani, Junaid Malik, Determination of lethal toxicity of copper to *Clarias gariepinus*, *IJARSE*, **4**, 1011 (2018).
18. Takeno, N. Atlas of Eh-pH diagrams (Intercomparison of thermodynamic databases). Geological survey of Japan open file report, 419, 1-287 (2005).
19. O. Plohl, M. Finšgar, S. Gyergyek, U. Ajdnik, I. Ban, L. Fras Zemljč, Efficient copper removal from an aqueous environment using a novel and hybrid nano-adsorbent based on derived-polyethyleneimine linked to silica magnetic nanocomposites, *Nanomaterial*, **9**, 209 (2019).
20. N. Sezgin, N. Balkaya, Adsorption of heavy metals from industrial wastewater by using polyacrylic acid hydrogel, *Desalination Water Treat.*, **57**, 2466 (2016).
21. M.N. Sahmoune, Evaluation of thermodynamic parameters for adsorption of heavy metals by green adsorbents, *Environ. Chem. Lett.*, **17**, 397 (2019).
22. I. Langmuir, The constitution and fundamental properties of solids and liquids, *J. Am. Chem. Soc.*, **38**, 2221 (1916).
23. H. Freundlich, Adsorption in solution, *Phys. Chem. Soc.*, **40**, 1361 (1906).
24. Y. Ho, G. McKay, Pseudo-second order model for sorption processes, *Process Biochem.*, **34**, 451 (1999).
25. Q. Hu, Z. Zhang, Application of Dubinin-Radushkevich isotherm model at the solid/solution interface: a theoretical analysis, *J. Mol. Liq.*, **277**, 646 (2019).
26. K.R. Hall, L.C. Eagleton, A. Acrivos, T. Vermeulen, Pore and solid diffusion kinetics in fixed-bed adsorption under constant pattern conditions, *Ind. Eng. Chem. Fundam.*, **5**, 212 (1966).
27. M. Temkin, V. Pyzhev, Recent modifications to langmuir isotherms, *Acta Phys. Chem.*, **12**, 217 (1940).
28. S. Mnasri-Ghnimi, N. Frini-Srasra, Removal of heavy metals from aqueous solutions by adsorption using single and mixed pillared clays, *Appl. Clay Sci.*, **179**, 105151 (2019).
29. I.M. Kenawy, M.A.H. Hafez, M.A. Ismail, M.A. Hashem, Adsorption of Cu(II), Cd(II), Hg(II), Pb(II) and Zn(II) from aqueous single metal solutions by guanlyl-modified cellulose, *Int. J. Biol. Macromol.*, **107**, 1538 (2018).
30. N. Samadi, R. Ansari, B. Khodavirdelo, Removal of copper ions from aqueous solutions using polymer derivations of poly(styrene-alt-maleic anhydride), *Egypt. J. Pet.*, **26**, 375 (2017).
31. E. Eskandari, M. Kosari, M.H.D.A. Farahani, N.D. Khiavi, M. Saeedikhani, R. Katal, M. Zarinejad, A review on polyaniline-based materials applications in heavy metals removal and catalytic processes, *Sep. Purif. Technol.*, **231**, 115901 (2020).
32. Y. Lin, H. Chen, K. Lin, B. Chen, C. Chiou, Application of magnetic particles modified with amino group to remove copper ions from aqueous solution, *J. Environ. Sci.*, **23**, 44 (2011).
33. G. Sharma, D. Pathania, M. Naushad, Preparation, characterization, and ion exchange behavior of nanocomposite polyaniline zirconium (IV) selenotungstos to phosphate for the separation of toxic metal ions, *Ionics*, **21**, 1045 (2015).
34. C. Liu, X. Liang, J. Liu, W. Yuan, Desorption of copper ions from the polyamine Functionalized adsorbents: behaviour and mechanism, *Adsorpt. Sci. Technol.*, **34**, 455 (2015).
35. S.R. Popuri, Y. Vijaya, V.M. Boddu, K. Abburi, Adsorptive removal of copper and Nickel ions from water using chitosan-coated PVC beads, *Bioresour. Technol.*, **100**, 194 (2009).
36. B. Houari, S. Louhibi, K. Tizaoui, L. Boukli-hacene, B. Benguella, T. Roisnel, V. Dorcet, New synthetic material-removing heavy metals from aqueous solution and wastewater, *Arab. Chem.*, **12**, 5040 (2019).
37. N. Rahman, N. Sato, S.Yoishioka, M. Sugiyama, H. Okebe, K. Hara, Selective Cu (II) adsorption from aqueous solution including Cu (II), Co (II) and Ni(II) by modified acrylic acid grafted PET (polyethylene terephthalate film), *Polym. Sci.*, **2013**, 798 (2013).
38. A. Celik, A. Demirbas, Removal and heavy metal ions from aqueous solution via Adsorption onto modified lignin from pulping waste, *Energy Source*, **27**, 1167 (2016).
39. O. Moradi, B. Mirza, M. Norouzi, A. Fakhri, Removal of Co (II), Cu (II) and Pb (II) ions by polymer based 2-hydroxyethyl methacrylate: thermodynamics and desorption studies, *J. Environ. Health Sci. Eng.*, **9**, 31 (2012).
40. Y. Yu, J.G. Shapter, R. Popelka-Filco, J.W. Bennett, A.V. Ellis, Copper removal using bio

- inspired polydopamine coated natural zeolites, *J. Hazard. Mat.*, **273**, 174 (2014).
41. W. O'Connell, C. Birkinshaw, T.F. O'Dwyer, A chelating cellulose Adsorbent for the removal of Cu (II) ion from aqueous solution, *J. Appl. Polym. Sci.*, **99**, 2888 (2006).
42. A. Aluigi, C. Tonetti, C. Vineis, C. Tonin, G. Mazzuchetti, Adsorption of copper (II) ions by keratin (PA6) blend nanofibers, *Eur. Polym. J.*, **47**, 1756 (2011).
43. H. Tu, M. Haung, Y. Yi, Z. Li, Y. Zhan, J. Chen, Y. Wu, X. Shi, H. Deng, Y. Du, Chitosan-rectorite nanospheres immobilized on polystyrene fibrous material via alternate electrospinning/electrospraying techniques for copper ions adsorption, *Appl. Surf. Sci.*, **426**, 545 (2017).
44. A. Mahapatra, B.G. Mishra, G. Hota, Electrospun Fe<sub>2</sub>O<sub>3</sub>-Al<sub>2</sub>O<sub>3</sub> nanocomposite fibers as an efficient adsorbent for removal of heavy metal ions from aqueous solution, *J. Hazard. Mater.*, **258**, 116 (2013).
45. G. Mohammadnezhad, P. Moshiri, M. Dinari, F. Steiniger, In situ synthesis of nanocomposite materials based on modified mesoporous silica MCM-41 and methyl methacrylate for copper (II) adsorption from aqueous solution, *J. Iranian Chem. Soc.*, **16**, 1491 (2019).
46. M. Dinari, G. Mohammadnezhad, R. Soltani, Fabrication of poly (methylmethacrylate)/Silica Kit-6 nanocomposite via in situ polymerization approach and their application for the removal of copper (II) ions from aqueous solution, *RSC Adv.*, **6**, 11419 (2016).
47. G. Mohammadnezhad, M. Dinari, R. Soltani, The preparation of modified boehmite/PMMA nanocomposite by in-situ polymerization and assessment of their capability for copper removal, *N. J. Chem.*, **40**, 3612 (2016).